doi.org/10.52568/001627/JCSP/47.01.2025

Synthesis of Calcium Oxide Nanoparticles, its Characterization, Effect on Soil pH and Kinetic Evaluation in Acidic Solution

[1]Patricia Ese Umoru, [2]Yusuf Sahabi, [3]Abdullahi Isah, [3]Aminu Aliyu, and [3]Ibrahim Dankane Bafarawa
[1,2]Department of Chemistry, Faculty of Science, Nigerian Defence Academy, Kaduna Nigeria.
[3]Department of Chemistry Federal College of Education Gidan Madi Sokoto, Nigeria
peumoru@nda.edu.ng

(Received on 10th March 2023, accepted in revised form 29th October 2024)

Summary: Synthesis of calcium oxide nanoparticles (CaO NPs), its characterization and kinetic evaluation with phosphite ion and soil sample in acidic solution was evaluated. CaO NPs was synthesized by thermal decomposition method at 850 ^{0}C for 6 hours using calcium carbonate ($CaCO_3$) as the raw material. The CaO nanoparticle was characterized by the use of X-ray Diffraction (XRD) and Scanning Electron Microscope (SEM). The sharp peak of CaO NPs was found to be between 17.98^o and 71.7^o with average crystallized particle sizes of 27.43 ± 0.1. The morphology was found to be a flower shape with agglomeration. The pace of the reaction was explored under specific concentration of hydrogen ion [H+], ionic strenght (I), and λ_{max} of 460 nm using spectrophotometric method. The stoichiometry of the reaction gave a mole ratio of 2:3 for PO_3^{3-} to CaO NPs. The reaction is 1st - order in favour of CaO and 1st – order in favour of PO_3^{3-}. Alteration of acid content decreased the pace of reaction. Addition of CaO NPs on the soil sample changed the pH from acidic to alkaline values ranging from 6.67 – 7.81. The administration of CaO NPs on acidic compound like soil will therefore improve the soil pH thereby boost the fertility of the soil. The experimental data showed that the reaction advanced via outer-sphere process.

Keywords: Synthesis, Characterization, Calcium oxide Nanoparticles, Soil pH, Phosphite ion (PO_3^{3-}).

Introduction

Nanoparticles are extremely small particles, usually with sizes between one and one hundred nanometers (nm). Materials at this scale have distinct biological, chemical, and physical characteristics that set them apart from their bulk counterparts. Nanoparticles are useful for a variety of applications in domains such as environmental research, electronics, and medicine because of these unique properties. Unique optical, electrical, and magnetic capabilities that are absent from bulk materials are frequently shown by nanoparticles. For example, localized surface plasmon resonance allows gold nanoparticles to show varying hues based on their sizes [1].

A number of variables can have great impact on the stability of nanoparticles, which includes temperature, pH, ionic strength, and the presence of stabilizers such as polymers or surfactants. Maintaining the stability of nanoparticles over time requires proper storage, which includes limiting temperature changes and avoiding light exposure [2].

Nanoparticles' effective shelf life can be greatly shortened by their propensity to agglomerate. A number of variables, including surface charge, pH, and the ionic strength of the dispersion medium, might affect aggregation. The stability and shelf life of nanoparticles can be impacted by storage circumstances such as humidity, light exposure, and temperature. For instance, high temperatures have the potential to quicken the degrading process [3, 4].

The dissolution of minerals in the soil with time may cause pH variations. For instance, the weathering of silicate minerals usually results in the release of alkaline ions, which usually raise the pH of the soil [5]. As time passes, the pH of the soil may drop as a result of organic matter breaking down and producing organic acids. The soil may become more acidic when organic matter builds up, particularly in wooded areas [6].

Calcium oxide Nanoparticles (CaONps) is a key compound because it is engaged as a catalyst in the industries, a powerful chemisorbent for harmful gases and used as calcitrant in paints, ceramics and other elementary utilization. Because of its various advantageous characteristics and uses in various industries, CaO nanoparticle has become a sign of considerable attention on a regular basis, Precipitation and thermal decomposition method for the synthesis of CaO nanoparticles are all known method of producing CaO nanoparticles that have good properties and characteristics that make it very useful [7]. Green nanoparticle synthesis is an environmentally acceptable technology that allows scientist all over the world to study the ability of various spices to create nanoparticle [8].

Phosphite is a component in the structure of plants which is responsible for the control of protein

*To whom all correspondence should be addressed.

synthesis. It plays an outstanding role within the growth of tissue and division of cells. Plants conduct complex energy transmissions, a function that needs phosphite [9]. The major source of inorganic phosphite fertilizers is rock phosphite. Phosphite is liable for variety of functions in plants which underlines its importance to plants. The growth of plants is boosted by the application of phosphite whose deficiency results in the weakness plants [10].

Shortage of phosphite is remedied by application of phosphite fertilizer on the soil. Plants grown using hydroponics may use phosphite solvated in water rather than adding it directly on the soil. The effect of the phosphite is the same, withstanding its application method [11]. Little is known on the kinetics of CaO NPs and phosphite ion in literature which prompted their evaluation.

Experimental

Synthesis and characterization of CaO Nanoparticles

The calcium carbonate ($CaCO_3$) sample was dried in an oven for 2 hours at 25 ^oC and grinded using vibrating cup mill machine for 3 minutes. The ground $CaCO_3$ was transferred in to a 32 mm sieving machine for 2 minutes and much fine powder was obtained from vacuum cleaner. The calcium carbonate powder was stored in a bottle for further analysis. Calcium oxide nanoparticles were synthesized from limestone by thermal decomposition method in which 35 g of the limestone fine powder was placed in a crucible, transferred into the furnace and heated at 850 ^oC for 6 hours eqn 1and a silver coloured powder was obtained. The resultant product obtained was characterized using XRD and SEM [12].

$$CaCO_{3(s)} \xrightarrow{850\ ^oC/6\ hrs} CaO\ Nps_{(s)} + CO_{2(g)} \quad (1)$$

X-ray Diffraction Analysis

Debye-Scherrer (equation 2) has been employed to calculate the particle sizes from the CaO NPs' line broadening.

$$D = \frac{K\lambda}{\beta Cos\theta} \quad (2)$$

where λ is X-Ray wavelength (1.5406 nm), β = FWHM (radian), θ = peak position and k = 0.94 (Scherrer constant).

Verification of Lambda Max (λmax)

The lambda max of the synthesized calcium oxide nanoparticles was obtained by recording its absorbance using Spectrum lab 725s spectrophotometer within a wavelength range of 200 – 800 nm [13].

Stoichiometric and Product Analysis

The concentration of calcium oxide nanoparticles (CaO Nps) was varied between (0.8 – 6) x 10^{-2} M (M = mol dm^{-3}) while that of (PO_3^{3-}) 2.0 x 10^{-2} M was kept constant at $[H^+]$ = 1.0 x 10^{-4} M, I = 1.0 M, T = 29.0 ± 0.1 ^OC. The reaction mixtures were monitored at λ_{max} = 460 nm. The constant values absorbance was plotted against the concentration of CaO nanoparticles and the spot at which the plot met was used to calculate the stoichiometry of the reaction [14]. A tiny portion of the reaction mixture was held up to a flame on a sanitized platinum wire. Furthermore, another portion of the reaction mixture was made acidic by adding a little amount of hydrochloric acid (HCl). The solution was then boiled slowly and treated with strong nitric acid, followed by a few drops of ammonium molybdate then heated to determine the product(s) of the reaction [15, 16] respectively.

Kinetics Experiment

All kinetic experiment was performed under pseudo first-order state in which the concentration of calcium oxide nanoparticle was made at least 10 - folds over that of the phosphite ion. The plot of log ($A_t - A_\infty$) against time (t) (where A_t and A_∞ are the absorbance at time, t and at infinity respectively) was carried out. The first-pace constant (k_1) was determined from the slope of the plots and the second - order pace constant (k_2) was determined from the relation: $k_2 = k_1/[CaO]$ nanoparticles [17]. The condition for the reaction [CaO NPs] = 2 x 10^{-2} M, $[PO_3^{3-}]$ = 2 x 10^{-3} M, $[H^+]$ = 1 x 10^{-4} M, I = 1.0 M, T = 29 ± 0.1 ^oC and λ_{max} = 460 nm.

Alteration of Acid Content

Alteration of acid content was investigated at constant concentrations of all other parameters such as [CaO NPs] = 2 x 10^{-2} M, $[PO_3^{3-}]$ = 2 x 10^{-3} M, I = 1.0 M, T = 29 ± 0.1 ^oC and λ_{max} = 460 nm while that of $[H^+]$ was varied between (1.0 – 6.0) × 10^{-4} M. Plots of k_2 against $[H^+]$ was carried out [18].

Effect of Ionic Concentration

Ionic concentration examination of the reaction medium was carried out in the range of (2.0 – 3.0) M (NaCl) while keeping the concentration of all other parameters constant. The swap in the ionic concentration was ascertained by plotting log k_2 versus √I as reported by [19].

Effect of Cation and Anion on the Pace of Reaction

The outcome of added ions on the pace of reaction was observed by the addition of various concentration of $[Mn^{2+}]$ = (0.5 – 2.5) x 10^{-2} M, (1.0 – 1.8) x 10^{-3} M of $[NO_3^-]$ and (1.0 – 3.0) x 10^{-2} M of $[Cl^-]$ while the concentrations of other reactants were kept constant at [CaO Nps] = 2 x 10^{-2} M, $[PO_3^{3-}]$ = 2.0 x 10^{-3}, I = 1.0 M, $[H^+]$ = 1.0 x 10^{-4} M, T = 29 ± 0.1 ºC and λ_{max} = 460 nm [20].

Effect of CaO NPs on Soil pH

Six (6) soil samples were collected from a farm land and air dried at room temperature for 2 days. Dried soil samples were pound into powder and filtered using a 2.0 µm mesh. Two (2 g) of the pulverized soil samples was transferred each into a 50 ml beaker tagged 1-6 containing 10 cm^3 of water and the pH were taken using a pH meter. CaO NPs was added to each beaker in the concentration range of (2.2 – 3.0) × 10^{-2} M.

Spectrum Inspection

The absorbance of the reaction mixture was taken after every five minutes after the commencement of the reaction. This was compared with the spectra of the calcium oxide nanoparticles over a wavelength range of 200 – 800 nm to determine if intermediate complex were formed or not during the period of the reaction [21].

Results and Discussion

X-ray Diffraction Analysis

The XRD results revealed that the CaO NPs synthesized were hexagonal in shape and the particle sizes were obtained from the line broadening. The extensive and sharp peak patterns revealed that the calcium oxide nanoparticles were well-crystallized in nature. The CaO NPs crystal size is between 17.9º to 71.7º (Fig. 1). The average crystallite yielded the value of 27.43 ± 0.1 nm. Accordingly, the calculated particle size evidently substantiated the average size of CaO Nps as less than 100 nm. Similar results have been reported by [22].

Scanning Electron Microscopy

The morphological analysis confirms that the image of CaO NPs showed agglomeration, revealing that the synthesized calcium oxide nanoparticles have a flower shape morphology with random arrangement as shown in Fig. 2.

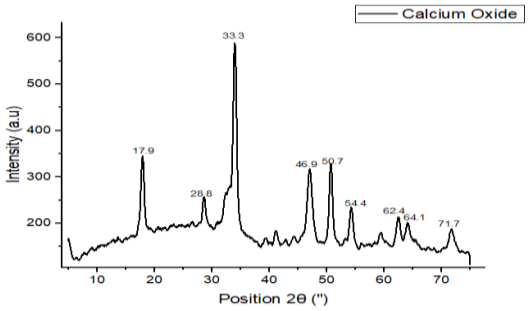

Fig. 1: XRD Pattern of Calcium Oxide Nanoparticles.

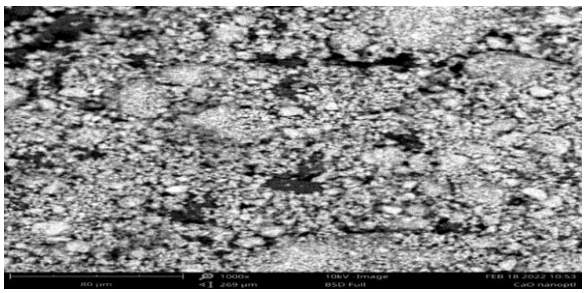

Fig. 2: SEM Image of CaO nanoparticles.

Verification of Lambda Max (λ_{max})

The λ_{max} of 460 nm was attained as shown in Fig. 3.

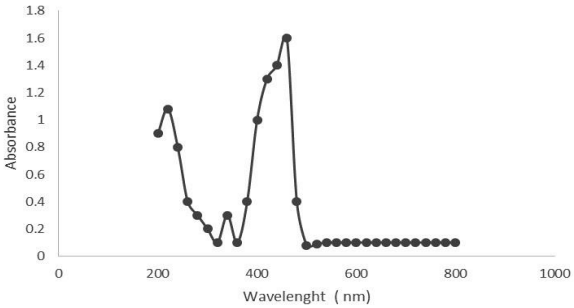

Fig. 3: Spectrum for CaO NPs owing Absorption Maxima.

Stoichiometry and Product Analysis

The stoichiometry results Fig. 4 showed that phosphite ion gave a mole ratio of 2 and 3 for calcium oxide nanoparticles. There was a distinctive orange-red glow that indicated the presence of calcium ions [15]. Phosphite ions are shown to be present by the production of a yellow precipitate called ammonium phosphomolybdate [16].

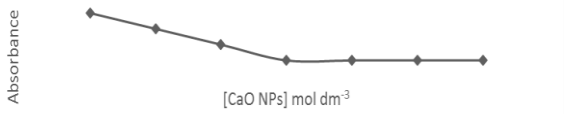

Fig. 4: Plot of absorbance versus [CaO nanoparticles] for the Determination of Stoichiometry of CaO NPs and PO_3^{3-} at [CaO] NPs = (0.8 – 2) x 10^{-2} M, $[PO_3^{3-}]$ = 2 x 10^{-2} M, $[H^+]$ = 1 x 10^{-4} M, I = 1.0 M, T = 29 ± 0.1 ^oC and λ_{max} = 460 nm.

This is in line with the stoichiometric equation presented in Eqn 3:

$$2PO_3^3 + 3CaONps + 6H^+ \longrightarrow Ca_3(PO_3)_2 + 3H_2O \quad 3$$

Kinetic Quantification

The pseudo – first order graph was straight line to more than 80 % range of the reaction which suggests a 1st - order dependence of rate on [CaO Nps] (Fig. 5). The second order - pace constant (k_2) is equitably constant (Table-1) which also reinforce 1st-order reaction. The slope acquired from the plot of log k_1 versus log [CaO NPs] (Fig. 6) was 1.0217 also stipulating 1st - order reliance on CaO NPs. The reaction is 2nd - order in general at constant $[H^+]$ concentrations [23].

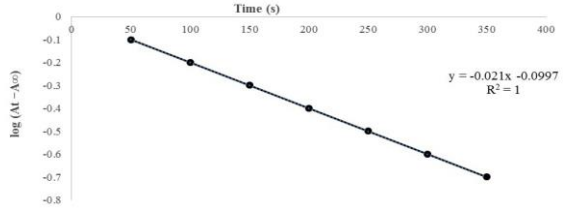

Fig. 5 Pseudo 1st – Order plot for the reaction of CaO NPs and PO_3^{3-} at [CaO NPs] = (1.0 - 6.0) x 10^{-2} M, $[PO_3^{3-}]$ = 2 x 10^{-3} M, $[H^+]$ = 1 x 10^{-4} M, I = 1.0 M, T = 29 ± 1.0 ^oC and λ_{max} = 460 nm.

log [CaO NPs]

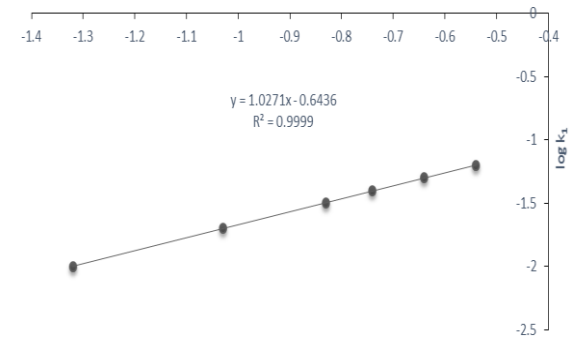

Fig. 6: Plot of log k_1 versus log [CaO NPs] at [CaO NPs] = (1.0 -6.0) x 10^{-2} M, $[PO_3^{3-}]$ = 2 x 10^{-3} M, $[H^+]$ = 1 x 10^{-4} M, I = 1.0 M, T = 29 ± 1.0 ^oC and λ_{max} = 460 nm.

Table-1: Pseudo – 1st – Order and 2nd – Order Pace Constants for the Reaction of CaO NPs and P_3O^{3-} [CaO NPs] = (1.0 -6.0) x 10^{-2} M, $[PO_3^{3-}]$ = 2 x 10^{-3} M, $[H^+]$ = 1 x 10^{-4} M, I = 1.0 M, T = 29 ± 0.1 ^oC and λ_{max} = 460 nm.

10^2 [CaO NPs] M	I M	10^4 $[H^+]$ M	10^2 k_1 s^{-1}	k_2 dm^3 mol^{-1} s^{-1}
1.0	**2.0**	**1.0**	**4.8**	**4.8**
2.0	**2.0**	**1.0**	**9.4**	**4.7**
3.0	**2.0**	**1.0**	**14.8**	**4.8**
4.0	**2.0**	**1.0**	**18.4**	**4.6**
5.0	**2.0**	**1.0**	**23.0**	**4.6**
6.0	**2.0**	**1.0**	**28.7**	**4.7**

Alteration of Acid Content on Reaction Pace

Alteration of acid content showed that the reaction pace decreased with increase in $[H^+]$ within the concentration span probed Table-2. This inverse relationship implies that there is deprotonation pre-equilibrium step and the pace determining step involves both the deprotonated and un-deprotonated species [24]. The slope obtained from the plot of k_2 vs $[H^+]$ (Fig. 7) was - 0.60 and an intercept of 4.80 stipulating negative 1st - order with respect to acid content. Application of CaO NPs on acidic medium like soil will therefore decrease its concentration.

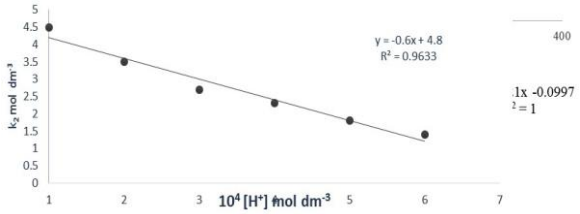

Fig. 7: Plot of k_2 versus $[H^+]$ for the Reaction of CaO Nps and PO_3^{3-} $[PO_3^{3-}]$ = 2 x 10-3 M, $[H^+]$ = (1.0 – 6.0) x 10-4 M, I = 1.0 M, T = 29 ± 0.1 ^oC and λ_{max} = 460 nm.

Table-2 Alteration of acid content of [CaO NPs] and PO_4^{3-} at $[PO_3^{3-}] = 2 \times 10^{-3}$ M, $[H^+] = (1.0 - 6.0) \times 10^{-4}$ M, I = 1.0 M, T = 29 ± 0.1 °C and λ_{max} = 460 nm.

10^2 [CaO NPs] M	I = M	10^4 $[H^+]$ M	$10^2 k_1 s^{-1}$	k_2 dm^3 mol^{-1} s^{-1}
1.0	2.0	1.0	9.1	4.5
1.0	2.0	2.0	6.9	3.5
1.0	2.0	3.0	5.4	2.7
1.0	2.0	4.0	4.6	2.3
1.0	2.0	5.0	3.8	1.8
1.0	2.0	6.0	2.9	1.4

Effect of Ionic Concentration

The pace of the reaction increased with increase in ionic concentration in the concentration span examined (Table-3) demonstrating positive salt effect. This shows that there may be presence of similar charged species during the formation of activated complex for the reaction. Positive value of the slope for the plot of log k_2 versus √I (Fig. 8) enfold the presence of two similar charged species at the pace determining step.

Table-3: Effect of Ionic Strength of the Reaction Medium on the Reaction pace for the Reaction of [CaO] NPs and PO_3^{3-} at $[PO_3^{3-}] = 2 \times 10^{-3}$ M, $[H^+] = 1.0 \times 10^{-4}$ M, I = (2.0 -3.0) M, T = 29 ± 1.0 °C and λ_{max} = 460 nm.

10^2 [CaO NPs] M	I M	$10^4[H^+]$ M	$10^2 k_1 s^{-1}$	k_2 dm^3 mol^{-1} s^{-1}
1.0	2.0	1.0	6.9	3.5
1.0	2.2	1.0	7.4	3.7
1.0	2.4	1.0	8.3	4.2
1.0	2.6	1.0	8.5	4.1
1.0	2.8	1.0	9.6	4.8
1.0	3.0	1.0	10.4	5.4

Table-4: shows that the soil pH values were acidic ranging from 4.08 – 4.98 but addition of CaO NPs on the soil samples changed the pH from acidic to alkaline values ranging from 6.67 – 7.81. This indicates that CaO NPs helps to improve soil pH and fertility.

Table-4: Effect of Added CaO NPs on soil Ph.

Soil Samples	pH	10^{-2} CaO NPs	pH
1	4.67	2.2	6.67
2	4.23	2.4	6.89
3	4.88	2.6	7.12
4	4.13	2.8	7.35
5	4.08	3.0	7.58
6	4.98	3.2	7.81

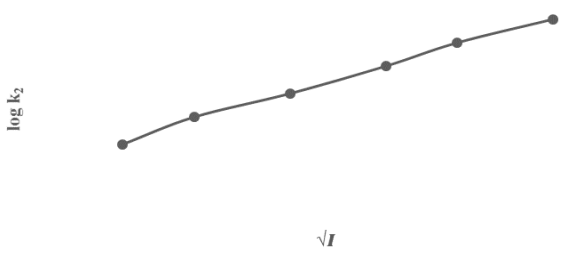

Fig. 8:: Plot of log k_2 versus √1 for the Reaction of CaO NPs and PO_3^3

Inspection of λ_{max}

Inspection of λ_{max} outcome showed no shift from the λ_{max} of 460 nm from the spectra of the reaction mixtures at five- minute interlude after the start of the reaction of CaO nanoparticles and PO_3^{3-} . Plot of $1/k_1$ versus 1/[CaO NPs] was linear which run through the origin Fig. 9.

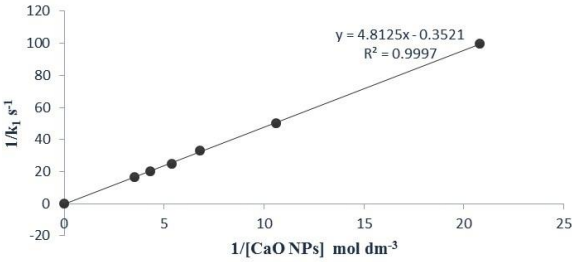

Fig. 9: Plot of $1/k_2$ versus 1/[CaO NPs].

Conclusion

The sharp peak of CaO NPs was found to be between 17.98° to 71.7° with average crystallized particles sizes of 27.43 ± 0.1 nm and the morphology were found to be flower shape with agglomeration. The pace of the reaction was found to be inversely dependent on acid content, $[H^+]$, increases with increase in ionic concentration on reaction medium. Application of CaO NPs on acidic medium like soil will therefore improve the soil pH thereby boost the fertility of the soil. The experimental data showed that the reaction advanced via outer-sphere mechanism.

Reaction Mechanism

Step-by-Step Mechanism

$$CaONps + H_2O \longrightarrow Ca^{2+} + 2OH^- \quad 4$$

$$PO_3^{3-} + 3H^+ \longrightarrow H_3PO_3 \quad 5$$

$$H_3PO_3 \rightleftharpoons H_2PO_3^- + H^+ \quad 6$$

$$H_2PO_3^- \rightleftharpoons HPO_3^{2-} + H^+ \quad 7$$

$$HPO_3^{2-} + PO_3^{3-} \longrightarrow 2PO_3^{3-} + H^+ \quad 8$$

$$2PO_3^{3-} + 3Ca^{2+} \longrightarrow Ca_3(PO_3)_2 \quad 9$$

$$H^+ + OH^- \longrightarrow H_2O \quad 10$$

Acknowledgement

The authors wish to acknowledge the Nigerian Defence Academy and the chemistry department for there support towards the success of this research.

Reference

1. L. M. Liz-Marzán, Gold nanoparticles: Synthesis and optical properties. *Inorg. Mater. Appl. Res*, **9**, 134 (2018).
2. S., Salem, et al. Nanomaterials: Types, Synthesis, Characterization, and Applications: A Comprehensive Review. *Biointerface Res. Appl. Chem.* **13**, 1 (2023).
3. Z. Huang, *et al*.**,** Strategies to Improve the Stability and Shelf Life of Nanoparticles: A Review. *J. Nanomater* (2021).
4. M. Vogt,, *et al*. Impact of Storage Conditions on the Stability of Nanoparticle Dispersions. *Mater. Today Commun*, **15**, 24 (2018)**.**
5. W. B. Miller, and R. L. Donahue, Soil pH and soil acidity, In Soil and Water Conservation for Productivity and Environmental Protection (1990).
6. W. B., McGill, and C. Figueiredo, Soil organic matter. In Soil Microbiology, Ecology, and Biochemistry (1993).
7. N. Gandhi, Y. Shruthi, G. Sirisha, and C. R Anusha, Facile and Eco-Friendly Method for Synthesis of Calcium Oxide (CaO) Nanoparticles and its Potential Application in Agriculture, *J. Life Sci*, **6,** 89 (2021).
8. S. K. Rinu, M. A. Queen and P. A. Upadhaya, Synthesis structural characterization and antibacterial applications of calcium nanoparticles, *J. Adv. Sci. Res*, **11,** 83 (2020).
9. M. Bucher, Functional biology of plant phosphate uptake at root and mycorrhiza interfaces. *J of New Phy.*, **173** 11 (2007).
10. F. E. Khasawneh, and E. C. Doll, The use of phosphate rock for direct application to soils, *Adv. Agron***, 30,** 159 (1979).
11. N. S. Bolan, R. E. White, and M. J. Hedley, A review of the use of phosphate rocks as fertilizers for direct application in Australia and New Zealand, *Aust. J. Exp. Agric*, **30**, 297 (1990).
12. F. Munawaroh, L.K. Muharrami, T. Triwikantoro and Z. Arifin, Calcium oxide characteristics prepared from ambunten's calcined limestone. *J P Sains*, **5**, 65 (2018).
13. I. U. Nkole, C. D. Osunkwo, AD. Onu, O. Onu, Kinetics and mechanism of the reduction of n-(2-hydroxyethyl)ethylenediaminetriacetatoiron(III) complex by thioglycol in bicarbonate buffer medium. *Int. J. Adv. Chem*, **6,** 102 (2018).
14. Y. N. Lohdip, A. P. Lungaka and J. J. Gongden, Kinetics and mechanism of the oxidation of tannic acid by potassium, *Niger. J. Chem. Res*, **84,** 465 (2021).
15. D. C. Harris, *Quantitative Chemical Analysis*. W. H. Freeman and Company (2015).
16. A. I. Vogel, *Vogel's Textbook of Quantitative Chemical Analysis*. Longman Scientific & Technical (1989).
17. I. Ibrahim, S. O. Idris, I. Abdulkadir and A. D. Onu, Kinetics and mechanism of the redox reaction of N, N′-phenylenebis-(salicylideneiminato) iron (III) with oxalic acid in mixed aqueous medium. *T M Chemistry*, **44,** 269 (2019).
18. Y. Ahmad, A. D. Onu, S. O. Idris, S. S. Iliyasu, Y. B. Abiti and U. Bello, The oxidation of ethylenediamine-N,N,N',N'-tetraacetatocobaltate(II) complex by hypochlorite ion in aqueous nitric acid medium. *ATBU J of Sc. Tech Ed*, **6,** 2277 (2018).
19. P. E. Umoru, H. A. Muhammad, Y. Sahabi and O. A. Babatunde, Investigation of the chemical reactions of 2, 4 , 6- trinitrophenol with thiocyanate ion in acidic condition, Kinetic Approach. *European J. Adv. Chem* **3,** 32 (2022).
20. Y. Mohammed, J. F. Iyun, S.O. Idris, Kinetic approach to the mechanism of the redox reaction of malachite green and permanganate ion in aqueous acidic medium. *AJPAC* **312**, 269 (2009).
21. O. A. Babatunde and O. N. Nwakama, Kinetic Approach to the Mechanism of Oxidation of L-Ascorbic Acid by Periodate Ion in Acidic Medium **42,** 32 (2013).
22. E. E. Khine, D. Koncz-Horvath, F. Kristaly, T. Ferenczi, G. Karacs, P. Baumli and G. Kaptay, Synthesis and characterization of calcium oxide nanoparticles for CO_2 capture, *J. Nanoparticle Res*, **24,** 8 (2022).
23. J. N. Edokpayi, J. F. Iyun and S.O. Idris, Kinetics and mechanism of electron transfer reaction between tetraoxoiodate(VII) ion and indigo carmine in aqueous hydrochloric acid medium, *J. Adv. Appl. Sci. Res.*, **2,** 1 (2011).
24. A. D. Onu, J. F. Iyun and S.O. Idris, The Kinetics of the Reduction of Tetraoxoiodate(VII) by n-(2-Hydroxyethyl)Ethylenediaminetriacetatocobaltate(II) Ion in Aqueous Perchloric Acid. *Transition Metal Chemistry*, **34,** 849 (2009).